



## Beef carcass microbiota after slaughtering and primary cooling: A metataxonomic assessment to infer contamination drivers

C. Botta<sup>a</sup>, I. Franciosa<sup>a</sup>, J.D. Coisson<sup>b</sup>, I. Ferrocino<sup>a</sup>, A. Colasanto<sup>b</sup>, M. Arlorio<sup>b</sup>, L. Cocolin<sup>a</sup>, K. Rantsiou<sup>a,\*</sup>

<sup>a</sup> Department of Agricultural, Forest and Food Sciences, University of Torino, Italy

<sup>b</sup> Dipartimento di Scienze del Farmaco – Università del Piemonte Orientale, Largo Donegani 2, I-28100 Novara, Italy

### ARTICLE INFO

#### Keywords:

Metataxonomic  
Culture-dependent methods  
Slaughterhouse microbiota  
Chemical analysis  
Beef carcasses

### ABSTRACT

The impact of primary cooling on beef microbiota was investigated on six beef carcasses consecutively processed with the parallel use of metataxonomic and culture-dependent analysis. Samples were collected immediately after slaughtering (AS) and after the 24th-hour post-cooling (PC) from three different surfaces, namely neck, flank and thigh.

The main objective was to examine whether the microbiota composition of beef carcasses changes as function of the surface sampled, primary cooling (from AS to PC) and animal's origin (breeder).

The outcomes underline that primary cooling did not affect qualitatively the composition of the potentially active microbiota or the carcass superficial counts. Although slight changes in chemical-physical parameters like volatile organic compounds (VOCs) were observed after cooling, the carcasses microbiota and its inferred metabolic pathways varied among animals as a function of their origin. Co-occurrence and co-exclusion analyses underlined competition for the colonisation of the carcass surface between *Brochothrix-Psychrobacter* and *Carnobacterium-Serratia-Pseudomonas*.

Once integrated in a comprehensive monitoring of the supply chain, the metataxonomic characterisation of the beef carcasses microbiota might represent a valid integrative approach to define the cuts' perishability and their appropriateness to specific packaging and storage methods. These new bits of knowledge could be the base to define good strategies for the prevention of meat spoilage.

### 1. Introduction

Processing of beef cattle is divided into two distinct phases; slaughtering of live animals and subsequent partitioning of the carcasses by boning, trimming, and eventually grinding. The primary cooling of the half carcasses provides the link between these two phases and likely represents the only step in which microbial contamination can be reduced or contained, especially when high chilling rate is applied (Liang et al., 2022). Indeed, after slaughtering a short-term storage in chiller rooms should reduce the temperature to  $\leq 7$  °C in the innermost point of the half carcass (EFSA, 2014a, 2014b). This primary cooling usually takes 24 h and can be sped up by ventilated chilling (Liang et al., 2022). Afterwards, chilled carcasses can undergo a traditional dry-aging lasting from 10 to 35 days. Alternatively, after the portioning, the primal cuts can mature in vacuum condition (wet-aging) or be directly processed through boning, trimming and mincing in the case of ground beef

(Kim et al., 2017).

In this frame, beef carcasses and products thereof are continuously exposed to an unavoidable microbial contamination until the final step of packaging and distribution in the retail markets (Kang et al., 2020). Primary contamination of the carcass by the autochthonous microbiome transmitted from the hides, a vector of faecal contamination too, occurs during skinning (Chopyk et al., 2016; Kang et al., 2019). By this initial contamination route, pathogens may also be transferred on the carcass surface and follow meat cuts along their shelf life (de Filippis et al., 2013). Secondary beef contaminations occur after the carcass cooling, along the phases of boning and final trimming-mincing prior to packaging (Kang et al., 2020). In this frame, it is not clear if the main contamination source can be the primary hide-to-carcass transmission or the subsequent cross-contamination mediated by surfaces, workers, and tools in contact with meat. As far as the secondary contamination is concerned, we should consider that boning, trimming, and grinding take

\* Corresponding author.

E-mail address: [kalliopi.rantsiou@unito.it](mailto:kalliopi.rantsiou@unito.it) (K. Rantsiou).

<https://doi.org/10.1016/j.foodres.2023.113466>

Received 20 June 2023; Received in revised form 29 August 2023; Accepted 10 September 2023

Available online 19 September 2023

0963-9969/© 2023 The Authors. Published by Elsevier Ltd. This is an open access article under the CC BY license (<http://creativecommons.org/licenses/by/4.0/>).

place in different slaughtering environments characterized by distinct resident microbial populations (Botta et al., 2020). Moreover, recent studies suggest that cross-contamination occurring during the final stages of trimming-grinding are mainly transitory and thus the product shelf life seems markedly dependent on the original contamination of the lot (Botta et al., 2022, 2021; Sade et al., 2017). Indeed, it has been demonstrated that different cuts share a common microbiota with the carcass section of origin, like a molecular signature that follows the final meat products along the shelf life (de Filippis et al., 2013).

The development of the beef carcasses microbiota strongly depends on environmental microbiota harboured in the abattoirs as well. In this frame, abattoirs can be summarily distinguished in relation to the supply chain as fragmented and integrated abattoirs (Kang et al., 2019). In the case of integrated supply chain, beef cattle are received from the same suppliers with minor variations in animal traits, whereas in the fragmented abattoirs animals are provided from multiple different breeders. This second case may result in herds of cattle with variations in physical traits such as weight, feed type and breed, as well as physiological and stress levels (Kang et al., 2020).

Taking into account the impact that different initial compositions of the carcass microbiota can exert on the final meat perishability, the current understanding of beef microbial contamination based on traditional microbiological methods does not seem sufficient to define the shelf life of the meat, or the shelf life of other similar minimally processed products (Duthoo et al., 2022; Esteves et al., 2021; Liang et al., 2022; Sade et al., 2017). There is a profound need of understanding not only surface contamination levels, but also changes in the carcass microbiota composition that may relate to chilling processes, origin and sampling area, or to the carcasses temporal-spatial proximity along slaughtering process (de Filippis et al., 2013; Stellato et al., 2016). The determination of carcass contamination can be certainly ameliorated by the use of metataxonomic analysis. Such use was proven beneficial in other animal science sectors connected to the cattle industry, such as those dealing with the assessment of dietary impact on ruminant microbiota and the evaluation of animal fertility (Kim, 2023; Poole et al., 2023).

Therefore, in this study, we applied metataxonomic and chemical analyses, coupled with bacterial counts, to understand the potential of such approach to discriminate between slaughtered beef carcasses and potentially help in defining the subsequent perishability of derived cuts and products.

## 2. Materials and methods

### 2.1. Beef carcass sampling and microbiological analysis

Three cattle (A, B, C) were consecutively slaughtered during the same production run (~100 heads/day processed) in a fragmented abattoir located in the Piedmont (North-West Italy) at the end of the slaughtering activity (Table 1). From each half carcass, three surface areas (100 cm<sup>2</sup>; ~1 cm of thickness; neck, flank and thigh; n = 6) were sampled with sterile sponges following UNI EN ISO 17604:2015 guidelines (Supplementary Fig. 1). In parallel, two samples adjacent to neck and flank sampling areas were collected with a scalpel (~100 cm<sup>2</sup>, ~1 cm of thickness). Collected samples were immediately vacuum

**Table 1**  
Characteristics of the three beef carcasses investigated.

Animal	Cattle Breed	Sex	Age (days)	Weight (kg)	Breeder	Slaughtering order
A	Valdostana Pezzata Nera	Male	624	258	Br1	1st
B	Mestizo	Male	626	424	Br2	2nd
C	Mestizo	Male	617	398	Br2	3rd

packed and stored at -20 °C for chemical analyses, while samples for microbiological analysis were transported in refrigerated conditions to the laboratory and analysed within four hours of sampling. Samplings were performed immediately after-slaughtering (AS) and after 24 h of cooling (post-cooling, PC). Primary cooling of beef carcasses was performed to reach a temperature throughout the meat not >7 °C (EFSA, 2014a, 2014b), by following the internal abattoir procedure (in a room at 2–4 °C for 24 h; conventional chilling rate ~1.5 °C/h).

Each superficial sample was aseptically trimmed (1–2 g pieces), mixed and 10 g of meat was diluted in 90 mL Ringer's solution (Oxoid). Serial dilutions were set up and microbial counts were performed for total viable count of mesophilic bacteria (TVC) and *Enterobacteriaceae* following UNI EN ISO 17604:2015 in the analytical laboratory of Laemmegroup S.r.l. (Tentamus Company, Moncalieri, Turin, Italy). An aliquot of 5 mL from each sample (first dilution) was centrifuged, the pellet was collected and stored with RNA-later (Ambion, Thermo Scientific, Milan, Italy) at -80 °C for subsequent RNA-extraction and amplicon-based sequencing analysis.

### 2.2. Proximate composition, FAME pattern, and peroxide values

The proximate composition determination was performed as described in previous work (Botta et al., 2021). The moisture, total nitrogen content and lipid fraction were determined using a Sartorius MA30 thermo-balance (Sartorius AG, Göttingen, Germany), a Kjeltac system I (Foss Tecator AB, Höganäs, Sweden), and a semiautomatic Soxhlet Büchi extraction system B-811 (Büchi Labortechnik AG, Flawil, Switzerland), respectively.

The analyses of fatty acids methyl esters (FAMES) and peroxide value were performed on the fat obtained from Soxhlet extraction, after removing the solvent. FAMES were obtained by transesterification of triglycerides as previously described (Locatelli et al., 2011) and then quantified via GC-FID, using a Thermo TRACE 1300 gas chromatograph, equipped with a FID detector and a split-splitless injector (Thermo Finningan, Rodano, Milan, Italy). The column was a DB23 (J&W Scientific): 30 m, inner diameter of 0.25 mm, and film thickness of 0.25 µm.

The gas carrier was hydrogen, applying a flux of 1.5 mL/min. The injector and the detector were operated at 250 °C and 350 °C, respectively, and the temperature ramp was 5 °C/min. The identification was obtained comparing the retention times from a mixture of 37 FAME standards (Supelco), and the standard chromatogram was reported in Supplementary Fig. 2.

A method, based on iron oxidation, was applied to determine the peroxide values, determining the absorbance at 500 nm (Shantha & Decker, 1994), by using a spectrophotometer (SHIMADZU UV-1900).

### 2.3. VOCs, amino acids and biogenic amines determination

The methods applied and extensively described in (Botta et al., 2021) were adopted here for the determination of Volatile Organic Compounds (VOCs), amino acids (AAs), and biogenic amines (BAs). The VOCs extraction was obtained via SPME, using a fiber coated with divinylbenzene/carboxy/polydimethylsiloxane (Supelco solid-phase micro-extraction [SPME] fiber assembly 50/30 µm DVB/CAR/PDMS) for their adsorption. A total of 1.5 g of fresh sample was inserted in a 10 mL vial, 50 µL of a 1 mg/L camphor solution was added as internal standard, and the vial was sealed with a cap fitted with a PTFE/silicone septum. The sample was incubated in a water bath at a temperature of 40 °C for 15 min, followed by the fiber exposition in the headspace at a temperature of 40 °C for 30 min.

For the GC-FID analysis a Thermo TRACE 1300 gas chromatograph (GC) (Thermo Finningan, Rodano, Milan, Italy) equipped with a FID and a split-splitless injector was used. The column was a low-polarity DB-5 (30 m by 0.25 mm by 0.25 µm) (J&W Scientific, Folsom, CA) for the GC analysis with 95 % dimethyl, 5 % phenyl, polymethylsiloxane stationary phase. The injector and the detector were operated at 250 °C and 350 °C,

respectively. Thermal desorption of the compounds from the SPME fiber was carried out in splitless mode (split flow = 12.0 mL/min; splitless time = 2 min). Hydrogen was the carrier gas with a constant flow rate of 1.2 mL/min. The oven was held at 50 °C for 2 min, then heated to 220 °C at a speed of 5 °C/min, kept constant for 5 min. The overall timing of the analysis was 41 min. The VOCs identification was obtained comparing the elution times and retention indexes of selected 11 standards (ethyl lactate, ethyl acetate, ethyl butyrate, ethyl hexanoate, benzaldehyde, hexanal, 1-pentanol, 1-hexanol, 2,3-butanedione, 3-methyl-1-butanol and acetoin). The quantities of the volatiles were estimated with that of the camphor internal standard using area normalization.

AAs and BAs were determined through HPLC-DAD, after their extraction with 5% trichloroacetic solution from the samples and subjected to a clean-up protocol as described in (Coisson et al., 2004). The standard solutions of amines and precursor amino acids were prepared by dissolving each compound in HPLC-grade water. The HPLC-DAD method, using a C18 reverse-phase Spherisorb S5 ODS 2 column (Phase Separation, Inc., Deeside, Clwyd, United Kingdom) (250-mm by 4.6-mm inner diameter, particle size 5 µm), applies a validated ion-pair method based on heptanesulphonate/phosphate buffer (KH<sub>2</sub>PO<sub>4</sub>) at pH 3.5. Pump A: Eluant 1 (heptanesulphonate: 10 mM; phosphate: 10 mM). Pump B: Methanol HPLC-grade. Gradient: 100 % pump A for 1 min; pump B from 0 to 26 % in 5.25 min; pump B from 26 to 35 % in 9 min; pump B from 35 to 42 % in 1.5 min; pump B at 42 % for 24 min; pump A at 100 % for 10.40 min. Flow-rate: 1 mL/min. Detection: (UV and DAD) 215 nm. The column was kept at 27 °C during the analyses (Coisson et al., 2004).

#### 2.4. RNA extraction, cDNA synthesis and amplicon-based sequencing

Total RNA extraction, cDNA synthesis and 16S rRNA gene amplification were performed as previously described (Botta et al., 2020).

The PCR products were purified utilising an Agencourt AMPure kit (Beckman Coulter, Milan, Italy), and the resulting products were tagged with sequencing adapters using the Nextera XT library preparation kit (Illumina Inc, San Diego, CA), according to the manufacturer's instructions. Sequencing was performed using a MiSeq Illumina instrument (Illumina) with V3 chemistry, which generated 2X250 bp paired-end reads. MiSeq Control Software, V2.3.0.3, RTA, v1.18.42.0, and CASAVA, v1.8.2, were used for the base-calling and Illumina barcode demultiplexing processes.

#### 2.5. Bioinformatic analysis

The 2,784,694 raw-reads obtained from 16S rRNA amplicon-based sequencing were analysed in R environment (R program version 4.1.1; <https://www.r-project.org>) using DADA2 package (Callahan et al., 2016). A total of 1,394,062 reads passed the quality filtering parameters applied [*truncLen* = *c*(250,236); *trimLeft* = *c*(36,36); *maxEE* = *c*(2,2); *minLen* = *c*(50,50)] with an average value of 40,002 reads/sample. After merging and *de-novo* chimera removal all paired-end sequences shorter than 344 bp were discharged: 88.4 % of the filtered sequences were used to construct the frequency table of Amplicon Sequence Variants (ASVs). All parameters not reported for filtering/merging steps are intended as default DADA2 setting.

Taxonomy was assigned with a confidence of 99 % sequence similarity through the Bayesian classifier method (Wang et al., 2007) by matching ASVs with 2021 release (version 138.1) of Silva prokaryotic SSU reference database (<https://zenodo.org/record/4587955#.YobFvhMzZRE>): the highest taxonomic rank level available was displayed if species was not reached. A following check at 100 % of similarity for species assignment was performed with *addSpecies* script. ASVs with uncertain taxonomic assignment (to the Order rank or lower resolution) were matched against NCBI nucleotide collection (<https://www.ncbi.nlm.nih.gov/>) and all sequences matching (>99 % similarity) to beef genomes or mitochondria-chloroplasts were removed from the frequency

tables.

ASVs were aligned with DECIPHER package and an unrooted phylogenetic tree was constructed with *phangorn* package (Schliep, 2011; Wright, 2016). Alpha diversity metrics (Observed Species, ACE, Shannon, Simpson, Fisher, PD whole tree) and weighted UniFrac beta-diversity distance were calculated with *phyloseq* and *picante* packages (Kembel et al., 2010; McMurdie & Holmes, 2013): rarefaction limit was set to the lowest number of sequences/sample.

Metagenome inference was performed from bacterial ASVs frequency table with MetGEMs toolbox (Patumcharoenpol et al., 2021) using default parameters (<https://github.com/yumyai/MetGEMs>) and AGORA collection as the reference database of genome-scale models (Magnúsdóttir et al., 2017). Gene family abundances were predicted and identified as KEGG orthologs (KO) and collapsed at level 3 of the KEGG annotations.

Sequencing data were deposited at the Sequence Read Archive of the National Center for Biotechnology Information under the bioproject accession number PRJNA940090.

#### 2.6. Statistics

Statistical analyses and data plotting were performed using R program, unless otherwise stated. Normality and homogeneity of the data (Log-Transformed abundances, alpha-diversity metrics, viable counts, chemical compounds concentrations) were checked by means of Shapiro-Wilk's W and Levene's tests, respectively. Variation and differences between multiple groups were assessed with one-way ANOVA (coupled with Tukey's post hoc test) and Kruskal-Wallis's test (coupled with pairwise Wilcoxon's test) for parametric and not parametric data, respectively. Pairwise comparisons were alternatively performed with Wilcoxon and T-tests according to data normality.

Principal Component Analysis (PCA) was performed on VOCs/FAA/BA concentrations with *factominer* package, while PCoA plot was produced from β-diversity weighted UniFrac distances. Non-metric Multi-Dimensional Scaling (NMDS) analyses were based on Bray-Curtis dissimilarities. The significant influence of factors like animal origins, phases (after slaughtering, post cooling) and sampling area (Neck, Flank, Thigh) on clusters produced in NMDS chart, PCA scores and PCoA were tested (individually or interactively) using the *Adonis* (PERMANOVA) function based on Bray-Curtis dissimilarity distance. Venn diagrams were constructed to study the number of shared and unshared taxa between animal, phases and sampling areas.

Correlation among taxa was computed by means of SparCC algorithm with default parameters and 100 bootstraps using the package *SpiecEasi* (Friedman & Alm, 2012). Pseudo *P*-values were calculated as the proportion of simulated bootstrapped and significant (pseudo-*P*-values < 0.001) correlations (positive: *R* > 0.4) were used to infer a co-occurrence network with the Gephi suite (version 0.9.2-beta; <https://gephi.org>). Presence of recurrent sub-networks modules (group of ASVs that are co-varying) was detected by the modularity algorithm (Blondel et al., 2008) implemented in Gephi suite with default parameters. Correlation between taxa (ASVs merged at highest taxonomic level achieved) and VOCs/FAA/BA concentration was performed by means of Spearman's rank correlation.

Enrichment analysis was performed with *GAGE* package on the predicted KO abundance table to identify biological pathways significantly overrepresented and underrepresented between batches (Luo et al., 2009).

### 3. Results

#### 3.1. Microbiological and compositional profiles after-slaughtering and post-cooling

The TVC indicating the superficial contamination of the carcasses did not differ among animals (Supplementary Table 1), while

*Enterobacteriaceae* were below the limit of detection in the majority of the samples ( $<2 \text{ Log CFU/dm}^2$ ). More importantly, the primary cooling did not affect at all the superficial TVC ( $P > 0.05$ ).

Concerning the proximate composition (moisture, total lipids and total proteins), we observed a high variability among sampling areas of the same animal and between different animals. The composition of the diacylglyceride fatty acid fraction permitted to cluster each carcass considering the specific fatty acid pattern influenced by the feeding of the animals (data not shown).

Instead, no differences among the three animals were underlined for amino acids (AA), biogenic amines (BA) and VOCs concentrations, although for each animal slight but significant differences between after-slaughtering (AS) and post-cooling (PC) samples were observed, particularly evident for AA and BA. The metabolism of amino acids can follow different routes, one of them is the decarboxylation forming biogenic amines. For this reason, we have quantified the presence of histamine and tryptamine in the samples. In detail from AS to the PC, histidine, phenylalanine and histamine showed significant increase in their concentrations in the animals A and B, whereas tryptophan and tryptamine significantly changed their concentration in the animals A and C (Fig. 1).

Concerning the VOCs, less evident differences were observed from AS and PC conditions (Fig. 1). Among alcohols, only 1-pentanol showed a significant increase in all three carcasses (T-test;  $P < 0.05$ ). Regarding esters, ethyl acetate and ethyl butyrate increased in post-cooling samples of animals A and C, respectively ( $P < 0.05$ ). The two identified ketones showed an opposite to each other trend, in details acetoin concentration increased in the samples of carcass A, while diacetyl decreased in B samples after cooling ( $P < 0.05$ ). In any case, the concentration of the VOCs was in all cases below the sensory perception thresholds.

The general tendency of most of VOCs, by considering each animal, was to increase in concentration after 24 h of cooling. The Principal Component Analysis (PCA) showed a partial (not significant) grouping of the samples related to the sampling time (AS or PC), but not between

the animals (Supplementary Fig. 3).

### 3.2. Microbiota composition and distribution

A total of 573 unique ASVs were overall detected in the 34 samples analysed. After the alignment at 99% of similarity to the Silva's reference database, 96% and 20% of the ASVs reached the taxonomic level of genus and species, respectively. The original ASVs were thus collapsed in 204 different taxa in relation to the higher taxonomic assignment obtained (Supplementary Table 2).

Proteobacteria and Firmicutes represented the more abundant phyla in the carcass's microbiota, followed by Actinobacteriota (Fig. 2 A and Supplementary Table 2). Going more deeply in the taxonomic assignments, *Burkholderiaceae*, *Moraxellaceae* and *Pseudomonaceae* families were the main Proteobacteria, while Firmicutes encompassed mostly *Carnobacteriaceae*, *Streptococcaceae* and *Listeriaceae* families. At the genus or species level we detected a core microbiota of eight taxa distributed in all three carcasses (A, B, C) and along the two temporal phases (AS, PC), namely: *Burkholderia* spp., *Carnobacterium divergens*, *Pseudomonas* (*P.*) *fragi*, *Brochothrix* (*B.*) *thermosphacta*, *Psychrobacter cibarius*, *Lactococcus* spp., *Achromobacter* spp. and *Stenotrophomonas maltophilia*.

Except for an overall abundance increase of the phylum Firmicutes after cooling (Wilcoxon's test;  $P$  [FDR]  $< 0.01$ ), the microbiota composition at the species-genus level differed significantly in relation to the animal of origin (Fig. 2 B), but was not affected by temporal phases or by the type of sampling area considered (Supplementary Table 3). Within the members of the core microbiota, *B. thermosphacta* and *P. fragi* were significantly more abundant in the carcasses A and A-B, respectively ( $P$ [FDR]  $< 0.001$ ). However, despite the three animal carcasses showing different microbial compositions, they were not representing three phylogenetically distinct microbial communities (weighted UniFrac distance; ADONIS and Anosim:  $P$ [FDR]  $> 0.001$ ).

As far as the taxa distribution is concerned (Fig. 2 C), in comparison with AS samples, we observed a higher number of taxa uniquely present

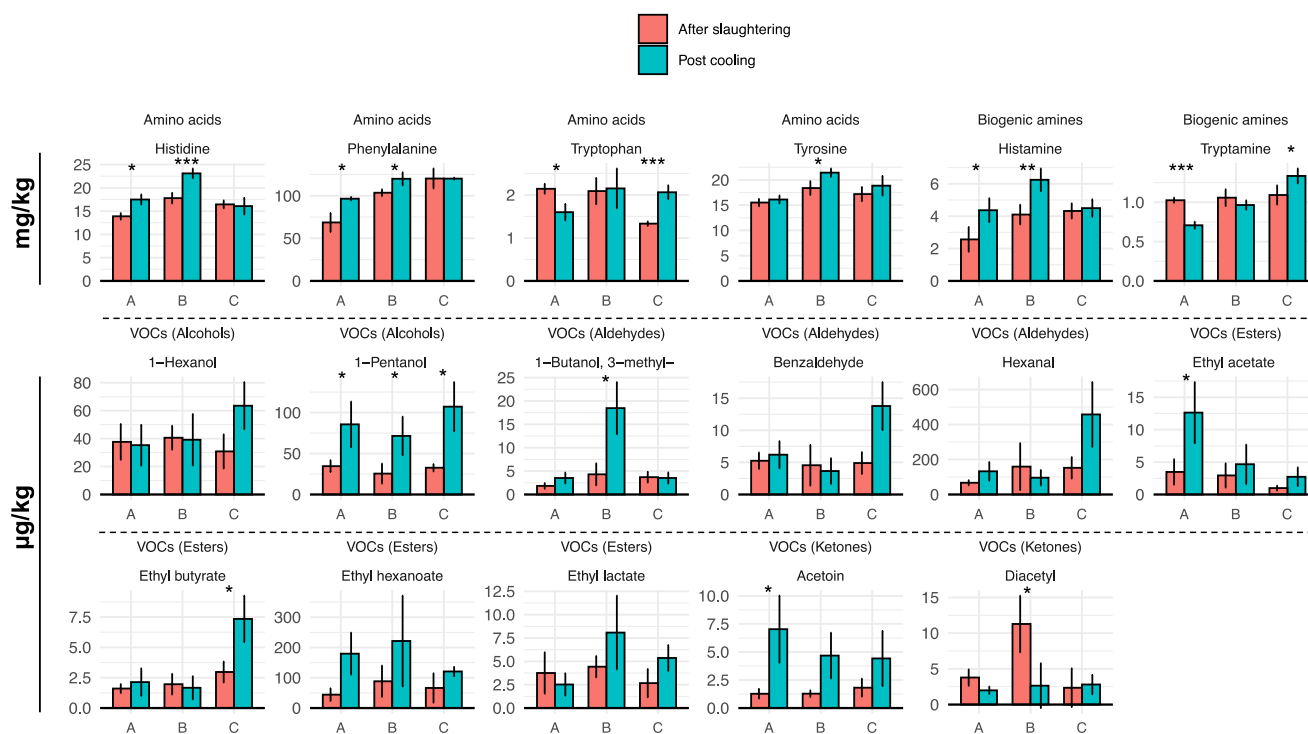


**Fig. 1.** Amino acids (AA), biogenic amines (BA) and Volatile Organic Compounds (VOCs) detected in beef carcasses. Bar plots displaying concentrations (mean  $\pm$  SD) of VOCs, AA and BA. Asterisks indicate significant differences between samples after slaughtering and post colling in each animal (Pairwise T-test; P-value: \* =  $<0.05$ ; \*\* =  $<0.01$ , \*\*\* =  $<0.001$ ).

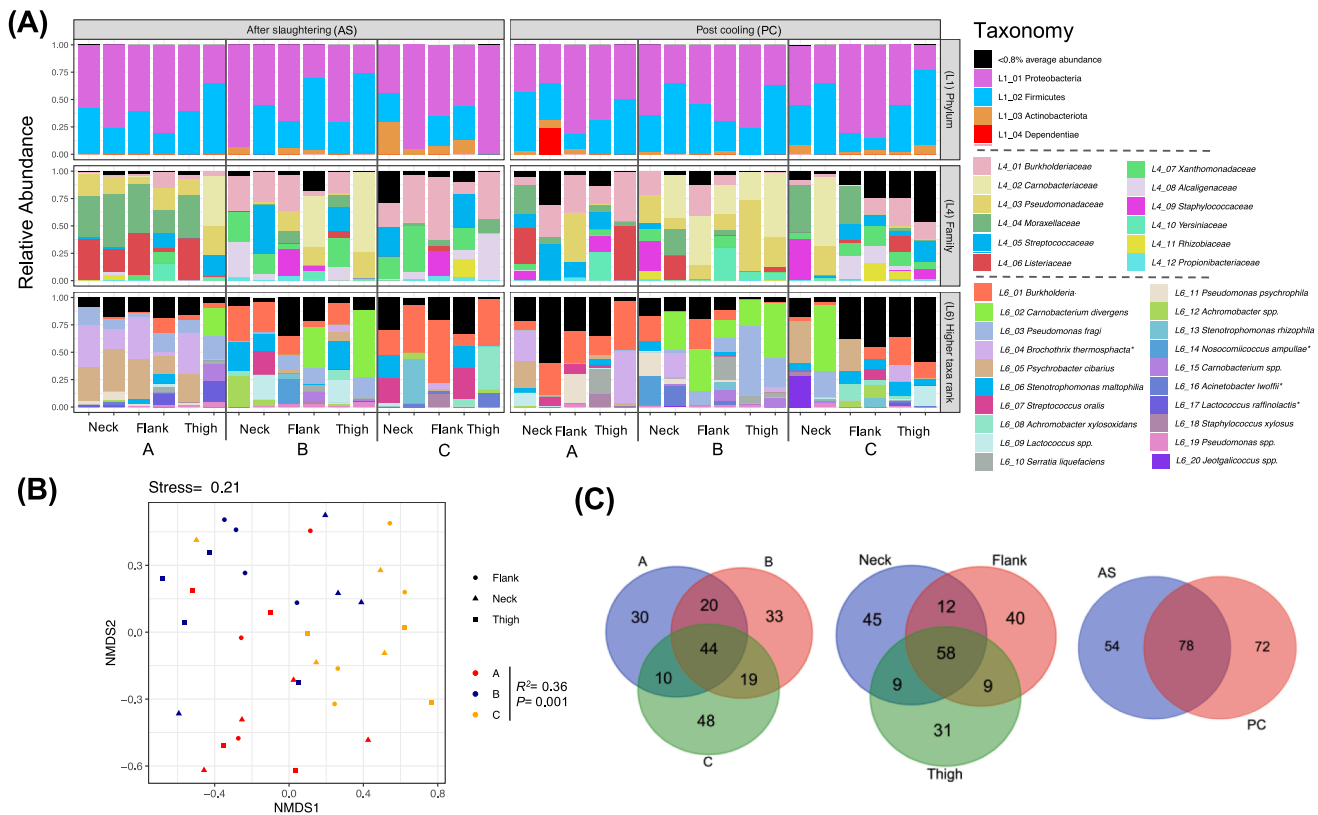


**Fig. 2. Microbiota composition after slaughtering and post cooling.** Stacked bar plots (A) showing microbiota composition (relative abundance) at different taxonomic rank levels and relative colour coding key. Samples are grouped by sampling time (after slaughtering, post cooling) and sequentially displayed according to animal and sampling area; taxa are sorted in the legend from the most to the least abundant. Biplot (B) of the Non-Multidimensional Scaling (NMDS) analysis coloured by animal origin, which significantly discriminated the samples (PERMANOVA;  $P < 0.001$ ). Venn diagrams (C) displaying the shared taxa between animals (A, B, C), temporal phases (AS, PC) and sampling areas (Neck, Flank, Thigh).

post-cooling (PC) and mainly represented by psychrotrophs. Moreover, an increasing number of taxa was detected from the upper to the lower sampling area of the carcasses, i.e., from the thigh to the neck. Changes observed in the microbiota distribution along phases and sampling areas did not determine anyway significant variations of the evenness and richness indices in alpha-diversity metrics ( $P[FDR] > 0.05$ ).

Concerning the direct links between bacteria abundances and AA/

BA/VOCs concentrations, *Carnobacterium spp.* was positively ( $Rho > 0.6$ ) correlated to 3-methyl-1-butanol. *Psychrobacter cibarius* and *Psychrobacter spp.* were negatively ( $Rho < -0.6$ ) correlated with this aldehyde, while *P. psychrophila* was negatively correlated with tryptamine concentration. Finally, *B. thermosphacta* presence was negatively correlated with the concentrations of phenylalanine, tyrosine and tryptamine (Supplementary Table 4).

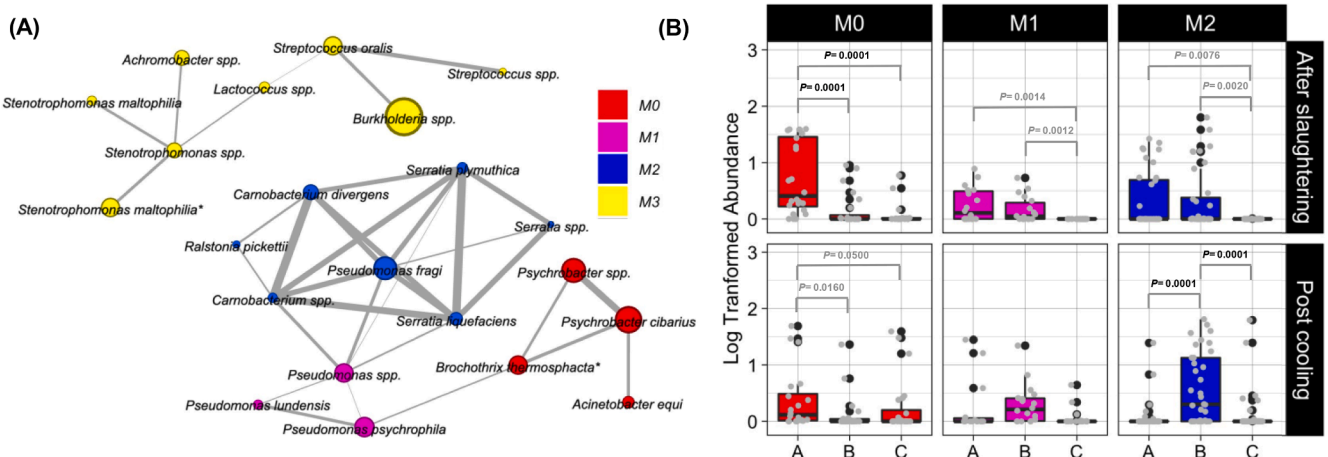


**Fig. 3. Co-occurrence network and metataxonomic signatures of animal carcasses.** Taxa (nodes) which are pairwise connected by lines (edges) in relation to significant SparCC correlation (100 bootstraps; pseudo- $P$ -value  $< 0.001$ ,  $R > 0.5$ ). Nodes are made proportional to taxa occurrences and coloured in relation to the co-occurring modules (A). Edges thicknesses are made proportional to SparCC correlation value. Box plots (C) displaying the modules distribution along the three animal carcasses (Kruskal-Wallis and Pairwise Wilcoxon tests, [FDR] adjusted).

### 3.3. Signatures of animal-related communities

In order to decipher the animal-related microbiota signatures, pairwise correlations were computed with SparCC algorithm and significantly positive ( $P$ -value < 0.001) correlations have been displayed in a network to highlight modules of highly co-occurring taxa (Fig. 3 A). Pairwise correlations were observed within and between members of Firmicutes and Proteobacteria phyla, and taxa belonging to the same genus co-occurred together, with the exception of genus *Pseudomonas*.

Seven taxa (nodes) included in the sub-network M3 are visibly segregated, although they cannot be considered part of a co-occurring module (M3 clustering coefficient = 0). All remaining 14 taxa are grouped in a second sub-network, which shows a clustering coefficient of 0.66 and harbours three distinguishable modules (M0, M1, M2) that segregate as a function of their distribution among carcasses and along the phases (Fig. 3 B). Indeed, module M0 shows that high co-occurrence of *B. thermosphacta* and *Psychrobacter spp.* is characteristic of the

carcasses A from the first sampling point after slaughtering. Members of *Carnobacterium*, *Serratia* and the *P. fragi* are all grouped in module M2, which is equally distributed in carcasses A and B after slaughtering, while in the post-cooling is uniquely associated to carcass B.

### 3.4. Inferred metabolic pathways

A total of 22 inferred metabolic pathways were differentially represented among the three animal carcasses in relation to the pairwise comparison of GAGE enrichment statistic ( $P < 0.001$ ). Amino acids and carbohydrate metabolisms were the more represented with 6 and 7 pathways differentially enriched, respectively (Fig. 4). Noteworthy, carcass A showed a great number of differentially enriched pathways in comparison with B (18 pathways) and C (17 pathways), while no pathways were differentially represented between B and C carcasses.

In particular, three pathways related to monosaccharides/sucrose/starch metabolisms and the central pathway of glycolysis/



**Fig. 4. Inferred metabolic pathways differentially represented in animal carcasses.** Results of pathways enrichment analysis with metabolic pathways significantly ( $g$ age enrichment statistic:  $P < 0.001$ ) overrepresented (green) and underrepresented (red). (For interpretation of the references to colour in this figure legend, the reader is referred to the web version of this article.)

gluconeogenesis were presumptively overrepresented in the microbiota of A and underrepresented in both microbiota of B and C carcasses. In parallel, the glyoxylate/dicarboxylate metabolism and the pathway responsible for propionic acid production (ko00650) were underrepresented in A. Differentially enriched pathways related to amino acid metabolisms were observed as well, with degradation pathways of lysine/valine/leucine and tryptophan/ $\beta$ -alanine metabolism enriched in B and C, and an overall higher biosynthesis of amino acids predicted for the microbiota of carcass A. Finally, lipopolysaccharide biosynthesis and fatty acid degradation were significantly enriched in B-C carcasses compared to A.

#### 4. Discussion

The beef carcasses are unique ecosystems, each one has its own microbiota influenced by the cross-contamination that occurs during events of the slaughtering process, like skinning and evisceration (Kang et al., 2020; Peruzy et al., 2021; Prache et al., 2022). Being the shelf-life of the meat strongly correlated with microorganisms able to colonize its surface, the total viable count (TVC) and *Enterobacteriaceae* loads are the most commonly used indices of the carcass contamination level, but they cannot provide detailed characterization of taxa potentially involved in spoilage (Braley et al., 2022; Liang et al., 2022). Therefore, metataxonomic snapshots of the microbial complexity in each carcass may represent a pivotal approach, together with the two above, to define its tendency to faster or slower spoilage (Stellato et al., 2016; Wheatley et al., 2014; Zwirzitz et al., 2020). Overall, the slaughtering process appears to cause a microbiota uniformization on the carcass surface. Afterward, only a small portion of these initial contaminant microbes will likely dominate and be part of the active spoilage microbiota in the final meat products, in relation to selective pressure exerted by the different storage conditions (Braley et al., 2022; Esteves et al., 2021; Stellato et al., 2016). In this frame, knowing the microbiota composition at the starting point of the meat supply chain may represent crucial information to define perishability of the derived products.

As first step, differences in the microbiota along the longitudinal carcass section have been sought, since higher microbial complexity has been previously observed in the anterior sides (de Filippis et al., 2013). This is due to the washing-driven migration of contaminant microbiota from the anus-thigh to the flank-neck areas, and is determined by the hooking position of the half-carcasses: from the hind legs during the entire slaughtering process. Herein, alpha- and beta-diversity parameters did not highlight such longitudinal variation, although in all three carcasses neck sampling areas harboured a greater number of unique taxa than flank and thigh.

Carcasses superficial contaminations were in the range of what was previously observed for beef (Kang et al., 2020), but no change in the microbial load along the primary cooling step was observed. Although the microbiota composition of the carcass is usually influenced by chilling (de Filippis et al., 2013; Liang et al., 2022; Wang et al., 2020), here this phenomenon was not evident, perhaps due to the limited timeframe monitored. Moreover, conventional cooling does not always reduce superficial contamination levels, and even an increased microbiota biodiversity can be observed after this step (Liang et al., 2022). In this study, an increase of species number from AS phase to PC was not observed, and the composition of carcasses microbiota was mainly influenced by the animal's origin. Some signatures of the different breeder of origin between carcasses A and B-C were found, like a peculiar presence of *Brochothrix* immediately after slaughtering and higher relative abundance of *Carnobacterium-Pseudomonas* in carcasses B and C. Moreover, different metabolic pathways have been inferred. In particular, a clear segregation as function of the breeder of origin was shown by the predicted microbiome, which highlighted distinct enriched pathways in carcass A compared to B-C. Different breeds, rearing methods and animal ages can determine significant differences in intestinal microbial populations of the animals, which in turn can be

transmitted directly or through dirty hides to the carcass (Braley et al., 2022; Wang et al., 2019; Yang et al., 2018). In this frame, the limited homogenization of the microbiota composition in three carcasses processed consecutively is somehow surprising, if we consider the sharing of the same environment, slaughtering tools, devices and surfaces of contact.

An interesting variation related to the time was the predominance of *Carnobacterium* in the carcass B after cooling. This spoilage associated lactic acid bacterium (LAB) has been found to be dominant in beef carcasses, but only in case of anaerobic cold storage (Esteves et al., 2021). The presence of this anaerobe may determine a possible higher perishability downstream in the supply chain, in case of final cuts or meat products stored under vacuum (Botta et al., 2022; Zhao et al., 2015). This is particularly true if we take in consideration the links between cuts and original carcasses (de Filippis et al., 2013), as well as the limited and transitory impact of final stages of meat manipulations like grinding (Botta et al., 2022, 2021). Based on the above, despite the equal counts level among the three carcasses, the carcass B showed after cooling a worrying metataxonomic profile in the prospect of an under vacuum packaging (VP) storage of its derived cuts or ground beef, likely more prone to spoilage (Botta et al., 2022; Casaburi et al., 2011). Although selective enumerations have not been performed in the current study, the extent to which amplicon sequencing targeting total RNA can realistically reflect variation of meat spoilage bacteria has been previously benchmarked and proven (Botta et al., 2020). Undoubtedly, all these considerations have to be confirmed in the context of a comprehensive metataxonomic monitoring of the entire beef supply chain, which considers every additional meat manipulation and productive environment that have an impact on the microbiota (de Filippis et al., 2013; Kaur et al., 2017; Stellato et al., 2016).

The co-occurrences and the related co-exclusions observed between two groups of major taxa, such as *Brochothrix-Psychrobacter* and *Carnobacterium-Serratia-P. fragi*, which respectively dominated the post-cooling microbiota of carcasses A and B, might perhaps indicate phenomena of antagonism and competition for the meat surface colonisation. Since the extent to which positive correlations among abundances reflects their ecological interactions is uncertain (Freilich et al., 2018), the taxa competition hypothesized here for carcasses and previously for the slaughterhouse environments need further confirmations (Botta et al., 2020). Taking into account the theoretical nature of our considerations, it is anyway noteworthy that co-exclusion mechanisms inferred from metataxonomic data and bacterial diversity have been shown to affect the fate of pathogens and spoilage bacteria inhabiting the final meat products (Zhang et al., 2022). For instance, a significant correlation has been revealed between low bacterial diversity and the presence of specific enterohemorrhagic *E. coli* serogroups or other faecal bacteria (Chopyk et al., 2016).

Differently from the microbiota composition, the concentration of some VOCs in the carcasses changed with time, showing a minimal but existing influence of the cooling process. Impact of the microbiota on the food spoilage can be investigated indirectly by characterising the meat volatile profile, which is influenced by the conditions of storage that modulate the meat microorganism growth (Húngaro et al., 2016; Kasper et al., 2012; Prache et al., 2022; Yang et al., 2022). An overall increase of VOCs concentrations was observed after the twenty-four hours of cooling, in which however the type of VOC involved differed among the three carcasses, except for 1-pentanol. This alcohol has been previously associated to the development of psychrotrophic LAB, such as *Lactococcus gasicomitatum* (Botta et al., 2018; Casaburi et al., 2015; Jääskeläinen et al., 2013). Therefore, its increase at low temperature is not surprising, although the specific associated taxon was not detected in the carcasses' microbiota. Moreover, significantly higher concentrations of acetoin were uniquely observed in the carcass A after cooling, albeit remaining below the perception threshold (Casaburi et al., 2015). This ketone confers an unpleasant buttery/creamy flavour to the meat, and its production has previously been associated with *Brochothrix thermosphacta*

(Ercolini et al., 2011; Ferrocino et al., 2013), which was indeed a predominant taxon in the microbiota of this carcass.

In summary, metataxonomic analysis of the carcasses microbiota here performed highlighted the impact of the carcasses' origin and the primary cooling performed after slaughtering. The need to introduce this NGS approach in the routine analysis for quality control and in parallel to culture-dependent analysis was further confirmed (Botta et al., 2022; Doulgeraki et al., 2012; Kang et al., 2020, 2019; Korsak et al., 2017). In detail, spoilage taxa from an animal hide colonise its carcass during high throughput slaughtering processes, and during the subsequent cooling and maturation period they have time to establish and adapt to the carcasses surfaces. The displacement of such ingrained microbiota by new environmental contaminants is unlikely to occur, or it represents a transitory modification in the microbiota composition of the final product (Botta et al., 2022). Despite the limited dimension of this study that cannot provide a conclusive response, the outcomes highlight how the metataxonomic analysis applied on carcasses, and downstream in the supply chain on primary cuts and products at the moment of packaging, would help to define the meat shelf-life. In particular, based on the initial carcass microbiota signature, the major or minor suitability to different packaging and storage conditions could be defined for the derived cuts, likely extending shelf-life and reducing waste products.

#### CRedit authorship contribution statement

**C. Botta:** Conceptualization, Investigation, Data curation, Formal analysis, Software, Writing – original draft. **I. Franciosa:** Formal analysis, Data curation, Software, Writing – original draft. **J.D. Coisson:** Investigation, Data curation, Conceptualization, Writing – review & editing. **I. Ferrocino:** Investigation, Writing – review & editing. **A. Colasanto:** Investigation, Writing – review & editing. **M. Arlorio:** Writing – review & editing. **L. Cocolin:** Writing – review & editing. **K. Rantsiou:** Conceptualization, Funding acquisition, Project administration, Writing - review & editing.

#### Declaration of Competing Interest

The authors declare that they have no known competing financial interests or personal relationships that could have appeared to influence the work reported in this paper.

#### Data availability

The sequencing data is available from a public database and the relative information is provided in the materials and methods section of the manuscript.

#### Acknowledgements

This study was funded by the Piedmont Region, Italy, through the P.O. R. FESR 2014-2020 financing system, under the European Commission decision no. C (2017) 6892. ("Meat Extend" project). The authors thank Daniele Sconfienza (Polo AGRIFOOD M.I.A.C. Scpa), Simonetta Riva (Veterinary Food Safety, Salmour, CN, Italy) and Barbara Rossi for their help during the samples collection.

#### Appendix A. Supplementary data

Supplementary data to this article can be found online at <https://doi.org/10.1016/j.foodres.2023.113466>.

#### References

- Blondel, V. D., Guillaume, J. L., Lambiotte, R., & Lefebvre, E. (2008). Fast unfolding of communities in large networks. *Journal of Statistical Mechanics: Theory and Experiment*, 10, 1–12. <https://doi.org/10.1088/1742-5468/2008/10/P10008>
- Botta, C., Coisson, J. D., Ferrocino, I., Colasanto, A., Pessione, A., Cocolin, L., ... Rantsiou, K. (2021). Impact of electrolyzed water on the microbial spoilage profile of Piedmontese steak tartare. *Microbiol. Spectr.*, 9, e01751–21. <https://doi.org/10.1128/Spectrum.01751-21>
- Botta, C., Ferrocino, I., Cavallero, M. C., Riva, S., Giordano, M., & Cocolin, L. (2018). Potentially active spoilage bacteria community during the storage of vacuum packaged beefsteaks treated with aqueous ozone and electrolyzed water. *International Journal of Food Microbiology*, 10–12. <https://doi.org/10.1016/j.ijfoodmicro.2017.10.012>
- Botta, C., Ferrocino, I., Pessione, A., Cocolin, L., & Rantsiou, K. (2020). Spatiotemporal distribution of the environmental microbiota in food processing plants as impacted by cleaning and sanitizing procedures: The case of slaughterhouses and gaseous ozone. *Applied and Environmental Microbiology*, 86, 1–15. <https://doi.org/10.1128/aem.01861-20>
- Botta, C., Franciosa, I., Alessandria, V., Cardenia, V., Cocolin, L., & Ferrocino, I. (2022). Metataxonomic signature of beef burger perishability depends on the meat origin prior grinding. *Food Research International*, 156, 1–13. <https://doi.org/10.1016/j.foodres.2022.111103>
- Braley, C., Fravallo, P., Gaucher, M. L., Larivière-Gauthier, G., Shedleur-Bourguignon, F., Longpré, J., & Thibodeau, A. (2022). Similar carcass surface microbiota observed following primary processing of different pig batches. *Frontiers in Microbiology*, 13. <https://doi.org/10.3389/fmicb.2022.849883>
- Callahan, B. J., McMurdie, P. J., Rosen, M. J., Han, A. W., Johnson, A. J. A., & Holmes, S. P. (2016). DADA2: High-resolution sample inference from Illumina amplicon data. *Nature Methods*, 13, 581–583. <https://doi.org/10.1038/nmeth.3869>
- Casaburi, A., Nasi, A., Ferrocino, I., Di Monaco, R., Mauriello, G., Villani, F., & Ercolini, D. (2011). Spoilage-related activity of *Carnobacterium maltaromaticum* strains in air-stored and vacuum-packed meat. *Applied and Environmental Microbiology*, 77, 7382–7393. <https://doi.org/10.1128/AEM.05304-11>
- Casaburi, A., Piombino, P., Nychas, G. J., Villani, F., & Ercolini, D. (2015). Bacterial populations and the volatiles associated to meat spoilage. *Food Microbiology*, 45, 83–102. <https://doi.org/10.1016/j.fm.2014.02.002>
- Chopyk, J., Moore, R. M., DiSpirito, Z., Stromberg, Z. R., Lewis, G. L., Renter, D. G., ... Wommack, K. E. (2016). Presence of pathogenic *Escherichia coli* is correlated with bacterial community diversity and composition on pre-harvest cattle hides. *Microbiome*, 4, 1–11. <https://doi.org/10.1186/s40168-016-0155-4>
- Coisson, J. D., Cerutti, C., Travaglia, F., & Arlorio, M. (2004). Production of biogenic amines in "Salamini italiani alla cacciatora PDO". *Meat Science*, 67, 343–349. <https://doi.org/10.1016/j.meatsci.2003.11.007>
- de Filippis, F., La Stora, A., Villani, F., & Ercolini, D. (2013). Exploring the sources of bacterial spoilers in beefsteaks by culture-independent high-throughput sequencing. *PLoS One*, 8, e70222.
- Doulgeraki, A. I., Ercolini, D., Villani, F., & Nychas, G. J. E. (2012). Spoilage microbiota associated to the storage of raw meat in different conditions. *International Journal of Food Microbiology*, 157, 130–141. <https://doi.org/10.1016/j.ijfoodmicro.2012.05.020>
- Duthoo, E., De Reu, K., Leroy, F., Weckx, S., Heyndrickx, M., & Rasschaert, G. (2022). To culture or not to culture: Careful assessment of metabarcoding data is necessary when evaluating the microbiota of a modified-atmosphere-packaged vegetarian meat alternative throughout its shelf-life period. *BMC Microbiology*, 22, 1–13. <https://doi.org/10.1186/s12866-022-02446-9>
- EFSA. (2014a). Scientific Opinion on the public health risks related to the maintenance of the cold chain during storage and transport of meat. Part 2 (minced meat from all species). *EFSA Journal*, 12, 1–30. <https://doi.org/10.2903/j.efsa.2014.3783>
- EFSA. (2014b). Scientific Opinion on the public health risks related to the maintenance of the cold chain during storage and transport of meat. Part 1 (meat of domestic ungulates). *EFSA Journal*, 12, 1–81. <https://doi.org/10.2903/j.efsa.2014.3601>
- Ercolini, D., Ferrocino, I., Nasi, A., Ndagijimana, M., Vernocchi, P., La Stora, A., ... Villani, F. (2011). Monitoring of microbial metabolites and bacterial diversity in beef stored under different packaging conditions. *Applied and Environmental Microbiology*, 77, 7372–7381. <https://doi.org/10.1128/aem.05521-11>
- Esteves, E., Whyte, P., Mills, J., Brightwell, G., Gupta, T. B., & Bolton, D. (2021). An investigation into the anaerobic spoilage microbiota of beef carcass and rump steak cuts using high-throughput sequencing. *FEMS Microbiology Letters*, 368, 1–10. <https://doi.org/10.1093/femsle/fnab109>
- Ferrocino, I., La Stora, A., Torrieri, E., Musso, S. S., Mauriello, G., Villani, F., & Ercolini, D. (2013). Antimicrobial packaging to retard the growth of spoilage bacteria and to reduce the release of volatile metabolites in meat stored under vacuum at 1°C. *Journal of Food Protection*, 76, 52–58. <https://doi.org/10.4315/0362-028X.JFP-12-257>
- Freilich, M. A., Wieters, E., Broitman, B. R., Marquet, P. A., & Navarrete, S. A. (2018). Species co-occurrence networks: Can they reveal trophic and non-trophic interactions in ecological communities? *Ecology*, 99, 690–699. <https://doi.org/10.1002/ecy.2142>
- Friedman, J., & Alm, E. J. (2012). Inferring correlation networks from genomic survey data. *PLoS Computational Biology*, 8, 1–11. <https://doi.org/10.1371/journal.pcbi.1002687>
- Húngaro, H. M., Caturla, M. Y. R., Horita, C. N., Furtado, M. M., & Sant'Ana, A. S. (2016). Blown pack spoilage in vacuum-packaged meat: A review on clostridia as causative agents, sources, detection methods, contributing factors and mitigation strategies.



- Trends in Food Science and Technology*, 52, 123–138. <https://doi.org/10.1016/j.tifs.2016.04.010>
- Jääskeläinen, E., Johansson, P., Kostianen, O., Nieminen, T., Schmidt, G., Somervuo, P., ... Björkroth, J. (2013). Significance of heme-based respiration in meat spoilage caused by *Leuconostoc gasicomitatum*. *Applied and Environmental Microbiology*, 79, 1078–1085. <https://doi.org/10.1128/AEM.02943-12>
- Kang, S., Ravensdale, J., Coorey, R., Dykes, G. A., & Barlow, R. (2019). A comparison of 16S rRNA profiles through slaughter in Australian export beef abattoirs. *Frontiers in Microbiology*, 10, 1–10. <https://doi.org/10.3389/fmicb.2019.02747>
- Kang, S., Ravensdale, J. T., Coorey, R., Dykes, G. A., & Barlow, R. S. (2020). Bacterial community analysis using 16S rRNA amplicon sequencing in the boning room of Australian beef export abattoirs. *International Journal of Food Microbiology*, 332, Article 108779. <https://doi.org/10.1016/j.ijfoodmicro.2020.108779>
- Kasper, J., Mumm, R., & Ruther, J. (2012). The composition of carcass volatile profiles in relation to storage time and climate conditions. *Forensic Science International*, 223, 64–71. <https://doi.org/10.1016/j.forsciint.2012.08.001>
- Kaur, M., Bowman, J. P., Porteus, B., Dann, A. L., & Tamplin, M. (2017). Effect of abattoir and cut on variations in microbial communities of vacuum-packaged beef. *Meat Science*, 131, 34–39. <https://doi.org/10.1016/j.meatsci.2017.04.021>
- Kemmel, S. W., Cowan, P. D., Helmus, M. R., Cornwell, W. K., Morlon, H., Ackerly, D. D., ... Webb, C. O. (2010). Picante: R tools for integrating phylogenies and ecology. *Bioinformatics*, 26, 1463–1464. <https://doi.org/10.1093/bioinformatics/btq166>
- Kim, M. (2023). Assessment of the gastrointestinal microbiota using 16S ribosomal RNA gene amplicon sequencing in ruminant nutrition. *Animal Bioscience*, 36, 364–373. <https://doi.org/10.5713/ab.22.0382>
- Kim, Y. H. B., Meyers, B., Kim, H. W., Liceaga, A. M., & Lemenager, R. P. (2017). Effects of stepwise dry/wet-aging and freezing on meat quality of beef loins. *Meat Science*, 123, 57–63. <https://doi.org/10.1016/j.meatsci.2016.09.002>
- Korsak, N., Taminiau, B., Hupperts, C., Delhalle, L., Nezer, C., Delcenserie, V., & Daube, G. (2017). Assessment of bacterial superficial contamination in classical or ritually slaughtered cattle using metagenetics and microbiological analysis. *International Journal of Food Microbiology*, 247, 79–86. <https://doi.org/10.1016/j.ijfoodmicro.2016.10.013>
- Liang, C., Zhang, D., Wen, X., Li, X., Chen, L., Zheng, X., ... Hou, C. (2022). Effects of chilling rate on the freshness and microbial community composition of lamb carcasses. *Lwt*, 153, Article 112559. <https://doi.org/10.1016/j.lwt.2021.112559>
- Locatelli, M., Coisson, J. D., Travaglia, F., Cereti, E., Garino, C., D'Andrea, M., ... Arlorio, M. (2011). Chemotype and genotype chemometrical evaluation applied to authentication and traceability of “tonda Gentile Trilobata” hazelnuts from Piedmont (Italy). *Food Chemistry*, 129, 1865–1873. <https://doi.org/10.1016/j.foodchem.2011.05.134>
- Luo, W., Friedman, M. S., Shedden, K., Hankenson, K. D., & Woolf, P. J. (2009). GAGE: Generally applicable gene set enrichment for pathway analysis. *BMC Bioinformatics*, 10, 1–17. <https://doi.org/10.1186/1471-2105-10-161>
- Magnúsdóttir, S., Heinken, A., Kutt, L., Ravcheev, D. A., Bauer, E., Noronha, A., ... Thiele, I. (2017). Generation of genome-scale metabolic reconstructions for 773 members of the human gut microbiota. *Nature Biotechnology*, 35, 81–89. <https://doi.org/10.1038/nbt.3703>
- McMurdie, P. J., & Holmes, S. (2013). Phyloseq: An R package for reproducible interactive analysis and graphics of microbiome census data. *PLoS One*, 8. <https://doi.org/10.1371/journal.pone.0061217>
- Patumcharoenpol, P., Nakphaichit, M., Panagiotou, G., Senavongse, A., Suratannon, N., & Vongsangnak, W. (2021). MetGEMs Toolbox: Metagenome-scale models as integrative toolbox for uncovering metabolic functions and routes of human gut microbiome. *PLoS Computational Biology*, 17, 1–18. <https://doi.org/10.1371/journal.pcbi.1008487>
- Peruzu, M. F., Houf, K., Joossens, M., Yu, Z., Proroga, Y. T. R., & Murru, N. (2021). Evaluation of microbial contamination of different pork carcass areas through culture-dependent and independent methods in small-scale slaughterhouses. *International Journal of Food Microbiology*, 336, Article 108902. <https://doi.org/10.1016/j.ijfoodmicro.2020.108902>
- Poole, R. K., Soffa, D. R., McAnally, B. E., Smith, M. S., Hickman-Brown, K. J., & Stockland, E. L. (2023). Reproductive microbiomes in domestic livestock: insights utilizing 16S rRNA gene amplicon community sequencing. *Animals*, 13. <https://doi.org/10.3390/ani13030485>
- Prache, S., Schreurs, N., & Guillier, L. (2022). Review: Factors affecting sheep carcass and meat quality attributes. *Animal*, 16, Article 100330. <https://doi.org/10.1016/j.animal.2021.100330>
- Sade, E., Penttinen, K., Björkroth, J., & Hultman, J. (2017). Exploring lot-to-lot variation in spoilage bacterial communities on commercial modified atmosphere packaged beef. *Food Microbiology*, 62, 147–152. <https://doi.org/10.1016/j.fm.2016.10.004>
- Schliep, K. P. (2011). phangorn: Phylogenetic analysis in R. *Bioinformatics*, 27, 592–593. <https://doi.org/10.1093/bioinformatics/btq706>
- Shantha, N. C., & Decker, E. A. (1994). Rapid, sensitive, iron-based spectrophotometric methods for determination of peroxide values of food lipids. *Journal of AOAC International*, 77, 421–424. <https://doi.org/10.1093/jaoac/77.2.421>
- Stellato, G., La Storia, A., De Filippis, F., Borriello, G., Villani, F., & Ercolini, D. (2016). Overlap of spoilage-associated microbiota between meat and the meat processing environment in small-scale and large-scale retail distributions. *Applied and Environmental Microbiology*, 82, 4045–4054. <https://doi.org/10.1128/AEM.00793-16>
- Wang, H., Qin, X., Li, X., Wang, X., Gao, H., & Zhang, C. (2020). Changes in the microbial communities of air- and water-chilled yellow-feathered broilers during storage at 2 °C. *Food Microbiology*, 87, Article 103390. <https://doi.org/10.1016/j.fm.2019.103390>
- Wang, Q., Garrity, G. M., Tiedje, J. M., & Cole, J. R. (2007). Naive Bayesian classifier for rapid assignment of rRNA sequences into the new bacterial taxonomy. *Applied and Environmental Microbiology*, 73, 5261–5267. <https://doi.org/10.1128/AEM.00062-07>
- Wang, X., Tsai, T., Deng, F., Wei, X., Chai, J., Knapp, J., ... Zhao, J. (2019). Longitudinal investigation of the swine gut microbiome from birth to market reveals stage and growth performance associated bacteria. *Microbiome*, 7, 1–18. <https://doi.org/10.1186/s40168-019-0721-7>
- Wheatley, P., Giotis, E. S., & McKeivitt, A. I. (2014). Effects of slaughtering operations on carcass contamination in an Irish pork production plant. *Irish Veterinary Journal*, 67, 1–6. <https://doi.org/10.1186/2046-0481-67-1>
- Wright, E. S. (2016). Using DECIPHER v2.0 to analyze big biological sequence data in R. *R J*, 8, 352–359. <https://doi.org/10.32614/rj-2016-025>
- Yang, H., Xiao, Y., Wang, J., Xiang, Y., Gong, Y., Wen, X., & Li, D. (2018). Core gut microbiota in Jinhua pigs and its correlation with strain, farm and weaning age. *Journal of Microbiology*, 56, 346–355. <https://doi.org/10.1007/s12275-018-7486-8>
- Yang, J., Yang, X., Lin, H., Liang, R., Niu, L., Zhu, L., ... Zhang, Y. (2022). Investigation of the relationship between microbiota dynamics and volatile changes in chilled beef steaks held under high-oxygen packaging enriched in carbon dioxide. *Meat Science*, 191, Article 108861. <https://doi.org/10.1016/j.meatsci.2022.108861>
- Zhang, P., Ruan, E., Holman, D. B., & Yang, X. (2022). Effects of a Carnobacterium maltaromaticum strain at natural contamination levels on the microbiota of vacuum-packaged beef steaks during chilled storage. *Lwt*, 168, Article 113944. <https://doi.org/10.1016/j.lwt.2022.113944>
- Zhao, F., Zhou, G., Ye, K., Wang, S., Xu, X., & Li, C. (2015). Microbial changes in vacuum-packed chilled pork during storage. *Meat Science*, 100, 145–149. <https://doi.org/10.1016/j.meatsci.2014.10.004>
- Zwirzitz, B., Wetzels, S. U., Dixon, E. D., Stessl, B., Zaiser, A., Rabanser, I., ... Selberherr, E. (2020). The sources and transmission routes of microbial populations throughout a meat processing facility. *npj Biofilms and Microbiomes*, 6, 1–12. <https://doi.org/10.1038/s41522-020-0136-z>